

CHAPTER FOUR

Bis-Polyamide-Intercalator Conjugates

The text of this chapter was taken in part from a manuscript co-authored with Ryan Stafford and Professor Peter B. Dervan (Caltech).

Fechter EJ, Stafford R, Dervan PB; Design of a Sequence-Specific Actinomycin D Mimetic, **2005**, *In preparation*.

Abstract

The natural product actinomycin D is a potent antitumor agent that binds DNA. The drug uses a single intercalator flanked by two minor-groove binding domains to preferentially target 5'-GC-3' sites and is generally regarded as cytotoxic. To extend the architecture of minor groove-binding intercalator conjugates that can utilize the polyamide scaffold, a sequence-specific analog of actinomycin D was created. A series of bis-polyamide-phenoxyazone conjugates were designed and synthesized where the natural product chromophore is tethered to two six-ring hairpin polyamides. The motif binds either a 12 bp or 14 bp site with higher affinity than a parent 6-ring polyamide control and maintains specificity over mismatch sites. The conjugate also unwinds DNA to approximately the same degree as actinomycin D, indicating an intercalative binding mode similar to the natural product. This approach to mimic DNA binding small molecules intercalators with programmable polyamides may be clinically useful in reducing cytotoxicity.

Introduction

Actinomycin D is a classic natural product isolated from *Streptomyces* that intercalates DNA base pairs with an aromatic phenoxazone chromophore and binds to the DNA minor groove with two coupled cyclic pentapeptide lactones (Figure 4.1).¹⁻⁷ The compound has a pseudo two-fold symmetry about the N10-O5 line of the phenoxazone ring

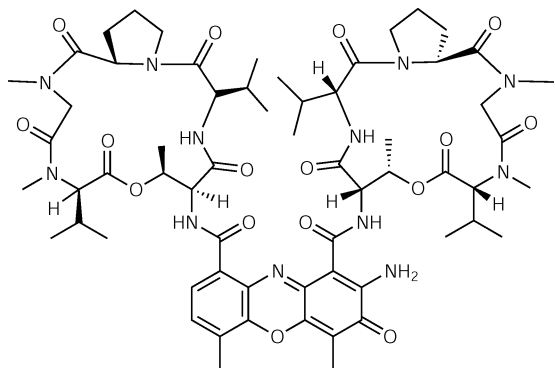


Figure 4.1 Chemical structure of Actinomycin D.

and binds DNA with a relatively high affinity ($K_a \sim 2.3 \times 10^6 \text{ M}^{-1}$)⁸ when compared to other mono-intercalators. Sobell and coworkers reported X-ray crystal structures for actinomycin D bound to deoxyguanosine where the compound intercalates between the 5'-GC-3' base pairs of d(ATGCAT)₂ from the minor groove and has a binding site size of 5-6 base pairs.^{9,10} Waring and coworkers performed DNase I footprint titration experiments which verified the preferred binding site d(GC)₂.¹¹⁻¹³ It's been postulated that the sequence preference derives from the threonine residues in the two macrocycles, which form specific hydrogen bonds to the guanine 2-amino group.^{9,10} Additionally, the GC base pair dipole moments are presumed to have a favorable interaction with the resonance charge distribution of the phenoxazone core (Figure 4.2).^{14,15}

Actinomycin D acts as potent antitumor agent known to inhibit DNA-directed RNA synthesis^{16,17} without inhibition of DNA replication¹⁸ – unlike other intercalating anticancer

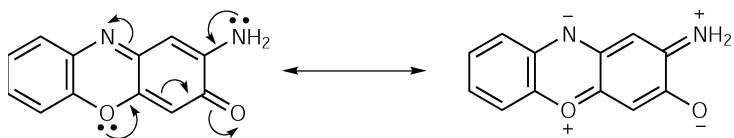


Figure 4.2 Resonance distribution of the phenoxazone chromophore.

drugs such as daunomycin (Chapter 1, Figure 1.3a), which inhibit both DNA transcription and replication. The drug also exhibits antibacterial activity, primarily against gram (+) bacteria, such as *B. Subtilis*, but has limited clinical use due to its extreme cytotoxicity.¹⁹ Despite the drug preference for GpC, numerous binding sites exist on any given DNA sequence, which may account for the pronounced toxicity. The design of a highly specific actinomycin D analog may provide insight into the importance of specificity on actinomycin's biological function.

In Chapter's two²⁰ and three,²¹ we explored the synthesis and binding properties of polyamide-acridine conjugates, which enforce different modes of binding while maintaining sequence-specificity and helix unwinding properties. Here we address the question of whether the DNA helix can accommodate an intercalator moiety covalently linked by two flanking minor groove-binding polyamides using actinomycin D as a base model.

We report here the synthesis of three bis-polyamide-phenoxazone conjugates **1-3** (Figures 4.3 and 4.4) and their abilities to specifically bind the minor groove of DNA. Minor groove-binding polyamides²² were used to replace the cyclic pentapeptides of actinomycin D. The key carbonyl amide recognition element of the threonine residues in actinomycin was preserved by linking the phenoxazone to the polyamide C-terminus with a glycine tether (Figure 4.3). The polyamide C-termini were varied in length using ethylene diamine, diamino propane, and diamino butane to link the polyamide core to the glycine tether. Binding studies were then completed using quantitative DNase I footprinting²³ on plasmids

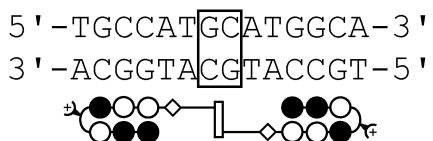
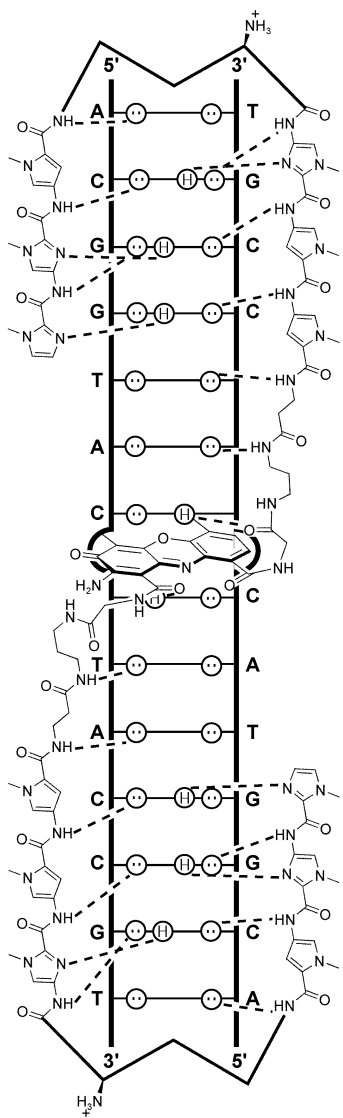


Figure 4.3 (Top) Hydrogen-bonding model of the twelve ring polyamide conjugate $\text{ImImPy-(R)}^{\text{H2N}}\gamma\text{-ImPyPy-}\beta\text{-C2-Phen-C2-}\beta\text{-PyPyIm-(R)}^{\text{H2N}}\gamma\text{-PyImIm}$ bound to the minor groove of 5'-TGCCATGCATGGCA-3'. Circles with dots represent lone pairs of N3 of purines and O2 of pyrimidines. Circles containing an H represent the N2 hydrogens of guanine. Putative hydrogen bonds are illustrated by dotted lines. (Bottom) Ball and stick model of the polyamide-conjugate binding its target site. Filled circles denote imidazole, open circles represent pyrrole, and the diamond represents β -alanine. The white bar depicts the acridine intercalator and the boxed region indicates the proposed intercalation site.

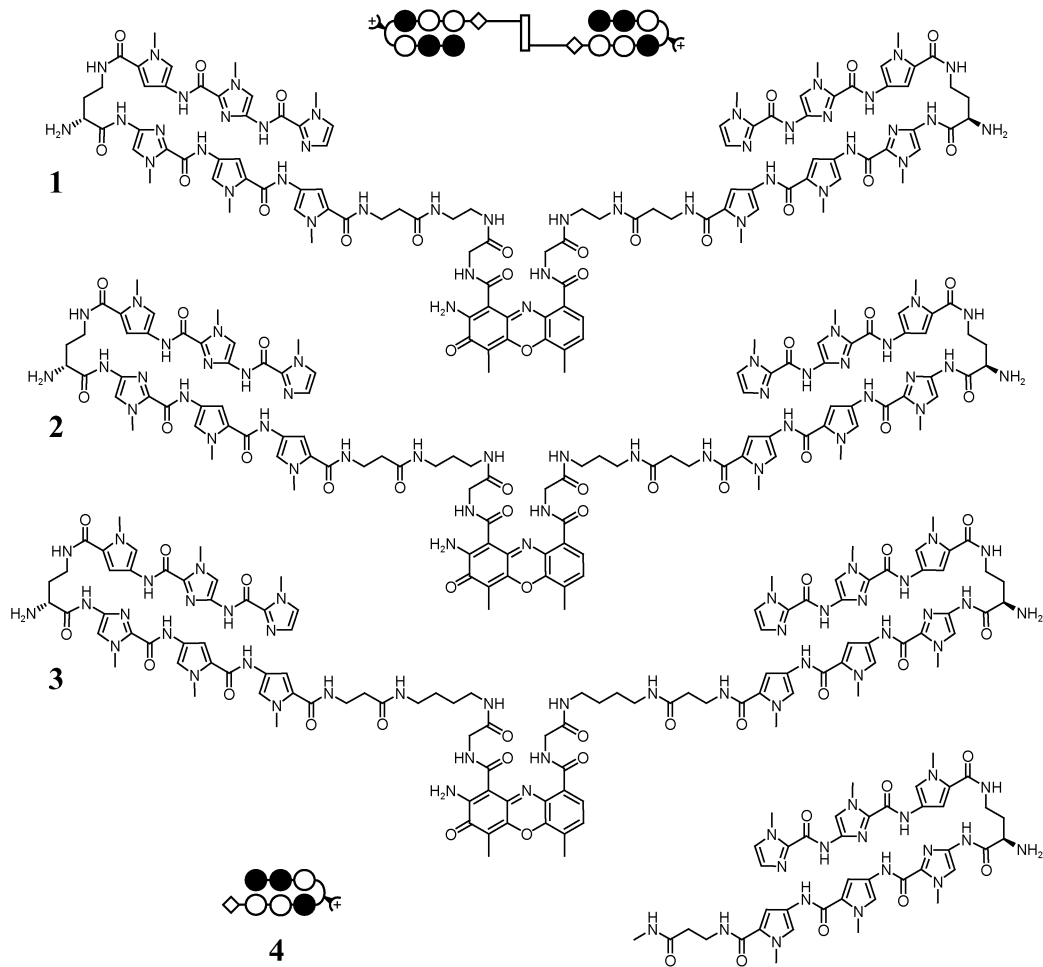


Figure 4.4 Structures of the tandem polyamide-intercalator conjugates (**1-3**) and control **4**.

containing either a 12-bp binding site (5'-WGCCWGCWGGC-3') or a 14-bp binding site (5'-WGCCWGCWGGC-3') to evaluate for the optimal binding site size. Each plasmid also contains a second binding site with a mismatch base pair under the polyamide binding regions and a third binding site with a mismatch under the proposed intercalation region in order to evaluate binding specificity. An intercalation unwinding angle was then determined using closed-circular DNA (ccDNA) methods developed by Crothers and Zeman.^{24,25}

Results

Synthesis of Polyamide-Acridine Conjugates 1-4

Twelve-ring hairpin polyamide conjugates containing the sequence ImImPy- $(R)^{\text{NHFmoc}}\gamma\text{-PyPyPy-}\beta\text{-Pam}$ -resin were synthesized in a stepwise manner on Boc- β -alanine Pam resin using established Boc-chemistry protocols.²⁶ The Fmoc-protected diaminobutyric acid (DABA) "turn" monomer was then deprotected by treatment with piperidine followed by reprotection with Boc₂O prior to polyamide aminolytic cleavage using one of three diamine linking agents (Figure 4.5). After reverse-phase HPLC purification, the polyamide primary amine was allowed to react with an activated carboxylate of the phenoxazone diacid 7 (generated in two steps from the glycine-linked 2-nitro-3-benzyloxy-4-methylbenzamide).²⁷ The crude material was then deprotected with trifluoroacetic acid (TFA) and the desired conjugate was purified by preparatory reverse-phase HPLC. A UV absorbance emission spectrum for **1** is shown in Figure 4.6.

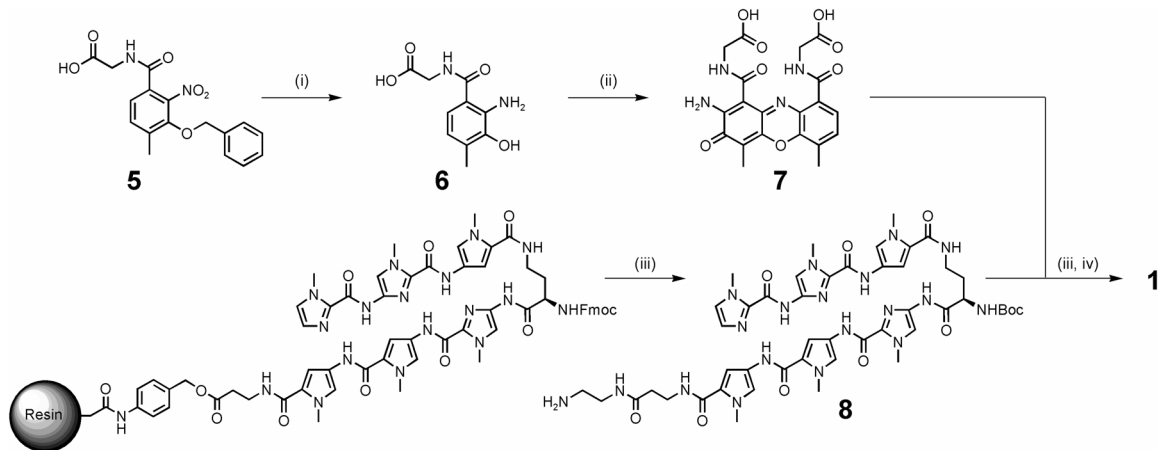


Figure 4.5 Synthetic scheme for bis-polyamide-intercalator conjugates: (i) Pd/C H₂ (1 atm, 3 h); (ii) K₃Fe(CN)₆ (1 h); (iii) 4:1 piperidine-DMF, 25°C (30 min); (iv) Boc₂O, DIEA, NMP, 55°C (30 min); (v) PyBop, DIEA (2 h) (vi) 80% TFA/DCM, 0.4 M PhSH, 25°C (15 min).

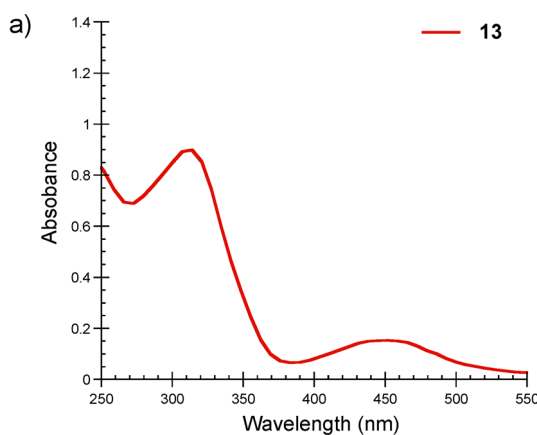


Figure 4.6 (a) Absorption spectra of free bis-polyamide-intercalator conjugate **1**.

Binding Energetics and Sequence Specificity

Quantitative DNase I footprint titrations were performed on a 5'-³²P-labeled PCR-amplified fragment of both pEF18 and pEF19 (Figure 4.7) to determine the equilibrium association constants (K_a) of polyamides **1-4** (Table 4.1) at different binding site sizes. The amplified fragment of pEF18 contains a 12 bp polyamide match site with an internal actinomycin D match site 5'-TGCCAGCTGGCA-3' (**I**), a 12 bp polyamide mismatch site with an internal actinomycin D match site 5'-TCCCAGCTGGGA-3' (**II**), and a 12 bp polyamide match site with an internal actinomycin D mismatch site 5'-TGCCATATGGCA-3' (**III**). The amplified fragment of pEF19 contains the same site arrangement as pEF18 except for the binding size which was increased to 14 bp. The control compound **4** contains a C-terminal methylamine tail and was used as a baseline for comparing binding energetics. Compound **4** bound both 12 bp match sites with modest affinities ($K_a = 2.4 \times 10^9 \text{ M}^{-1}$ and $4.0 \times 10^9 \text{ M}^{-1}$ for sites **I** and **III**, respectively). As expected, affinities of the unlinked control did not significantly change when bound to the 14 bp match sites ($K_a = 3.1 \times 10^9 \text{ M}^{-1}$ and $6.0 \times 10^9 \text{ M}^{-1}$ for sites **I** and **III**, respectively). The slightly higher affinities observed at match site

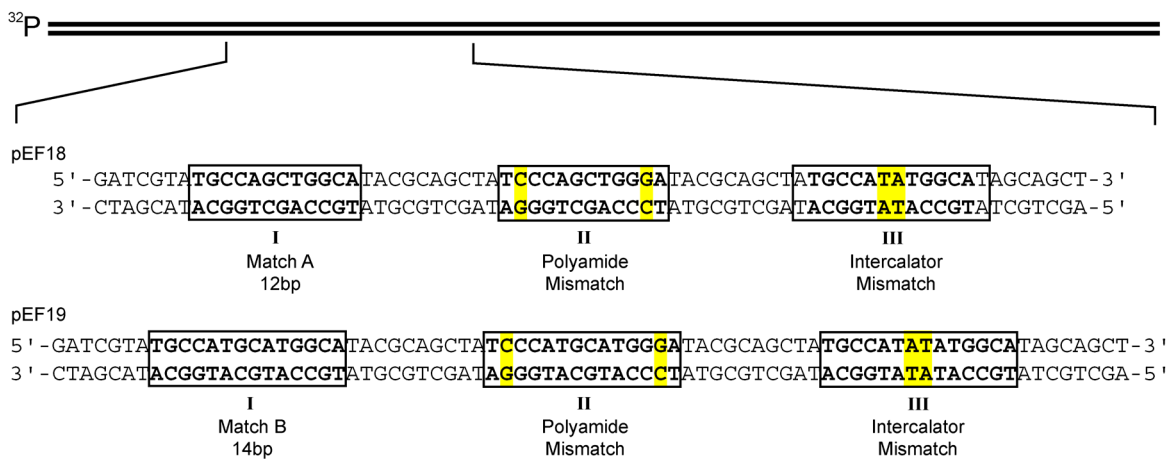


Figure 4.7 Sequence of the synthesized inserts for plasmids containing the 12 bp binding site (pEF18) and 14 bp binding site (pEF19). Target sites are shown in boxes, and mismatch sites are shaded with yellow.

III are rationalized by the steric incompatibility of a neighboring exocyclic NH_2 of guanine flanking the methyl amine tail of **4**. All three conjugates **1-3** bind to match sites **I** and **III** of both plasmid sequences with equal or greater affinity than the control **4** (Table 4.1). Compound **1** bound to the 12 bp match site **I** with the highest affinity ($K_a = 1.4 \times 10^{10} \text{ M}^{-1}$), roughly six-fold higher than the control (see Figure 4.8), and showed no discrimination over the two base pair substitution of match **III** ($K_a = 1.1 \times 10^{10} \text{ M}^{-1}$). For the 14 bp sequence, compound **2** bound with the highest affinity ($K_a = 2.2 \times 10^{10} \text{ M}^{-1}$) to match **I**, approximately 8-fold higher than the control and once more showed no discrimination over match **III**. Interestingly, compound **1** bound match site **I** on the 14 bp sequence with a 10-fold lower affinity than match site **III**. It appears the presence of the exocyclic amine contained by the GC base pair prevents binding of this compound to the larger site. It's possible that the intercalator and minor groove-binding moieties have reached maximum extension with the 14 bp match **III**, and that the additional bulk of the GC base pairs from match **I** causes the important specific hydrogen bonding contacts to be dislocated. The lack of specificity between match sites **I** and **III** for the conjugates suggests that the glycine carbonyl is not properly oriented to permit sufficient hydrogen bonding to the exocyclic nitrogen of guanine.

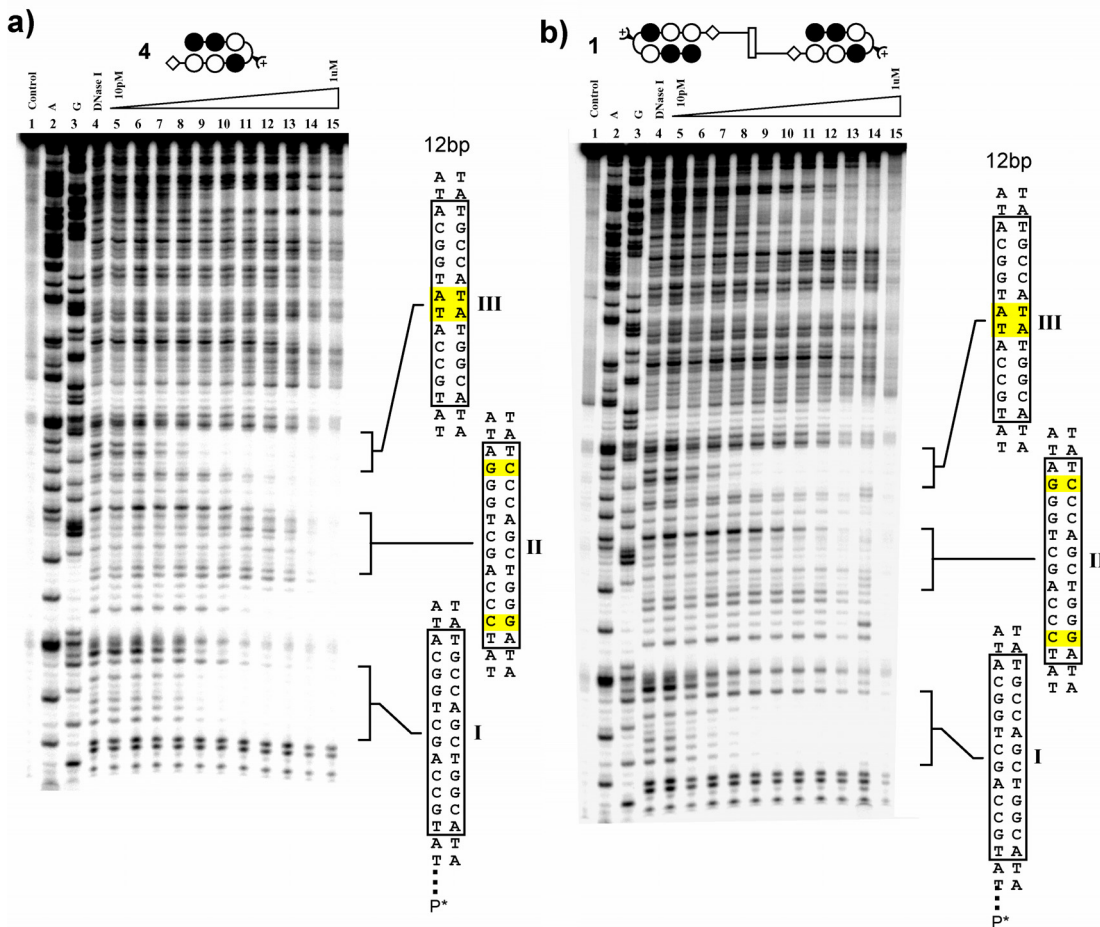


Figure 4.8 Quantitative DNase I footprint titration experiments with (a) $\text{ImImPy-(R)}^{\text{H2N}}\gamma\text{-PyPyPy-}\beta\text{-Me}$ (**4**) and (b) $\text{ImImPy-(R)}^{\text{H2N}}\gamma\text{-ImPyPy-}\beta\text{-C2-Phen-C2-}\beta\text{-PyPyIm-(R)}^{\text{H2N}}\gamma\text{-PyImIm}$ (**1**) on the PCR-amplified 5'-³²P-labeled fragment of pEF18. **I**, **II**, and **III** correspond to the sites indicated in Figure 4.6: Lane 1, intact DNA; lane 2, A reaction; lane 3, G reaction; lane 4, DNase I standard; lanes 5, 6, 7, 8, 9, 10, 11, 12, 13, 14, and 15, 10 pM, 30 pM, 100 pM, 300 pM, 1 nM, 3 nM, 10 nM, 30 nM, 100 nM, 300 nM, and 1 μ M polyamide, respectively. All reactions contain 15 kcpm amplified fragment, 10 mM Tris-HCl (pH 7.0), 10 mM KCl, 10 mM MgCl₂, and 5 mM CaCl₂.

Nonetheless, binding over two running GC base pairs in match site **I** is tolerated for all conjugates in the series (apart from conjugate **1**) contrary to typical polyamide linker selectivity. All compounds showed only slight binding to the mismatch site **II**, indicating that the linked conjugates maintain their specific binding characteristics to DNA.

Helical Unwinding Angle Determination

To confirm intercalation and quantitatively measure the unwinding effects of the twelve-ring bis-polyamide-phenoxyazone conjugates, compound **1** was selected for a helical

Table 4.1 Equilibrium Association Constants (M^{-1})^a

polyamide	GC Match I (12bp)	AT Match II (12bp)	GC Match I (14bp)	AT Match II (14bp)
1	1.4×10^{10}	1.1×10^{10}	2.3×10^9	2.0×10^{10}
2	7.9×10^9	8.6×10^9	2.2×10^{10}	2.0×10^{10}
3	4.6×10^9	4.9×10^9	7.9×10^9	4.5×10^9
4	2.4×10^9	4.0×10^9	3.1×10^9	6.0×10^9

^a The reported association constants are the average values obtained from three DNase I footprint titration experiments. The standard deviation for each data set is indicated in parentheses. Assays were performed at 22°C at pH 7.0 in the presence of 10 mM Tris·HCl, 10 mM KCl, 10 mM MgCl₂, and 5 mM CaCl₂.

unwinding assay using closed-circular pUC19 DNA.^{24,25} Relaxation reactions were carried out on pUC19 preequilibrated with varying concentrations of polyamides²⁸ or pUC19 alone. Following topoisomerase I (Topo I) treatment and extraction of intercalated conjugate, the two-dimensional (2D) agarose gel electrophoresis of ccDNA for all reactions containing conjugate **1** resulted in a primarily negative distribution of topoisomers, while control experiments lacking polyamide resulted in a primarily positive distribution of topoisomers. The differences in distribution maxima were compared mathematically (see experimental) and show decreasing apparent unwinding angles (ϕ_{ap}) for simultaneously decreasing conjugate and plasmid concentrations (Figure 4.9). The actual unwinding angle (ϕ), determined from the ordinate intercept in Figure 4.9, is 28°.

The unwinding assay provides evidence that a bis-polyamide-phenoxazone conjugate can intercalate while binding to the minor groove. Since parent hairpin polyamides have little effect on DNA unwinding,^{29,30} the total unwinding is attributed to the tethered intercalating moiety or distortion caused by non-optimal linkage to the polyamide. The helical unwinding angle (ϕ) for conjugate **1** is consistent with reported values for the unconjugated actinomycin D (26° found by analytical ultracentrifugation of ligand bound to ϕ X174 RF DNA),³¹ indicating that minimal distortion is induced on the helix by the linked hairpin polyamides.

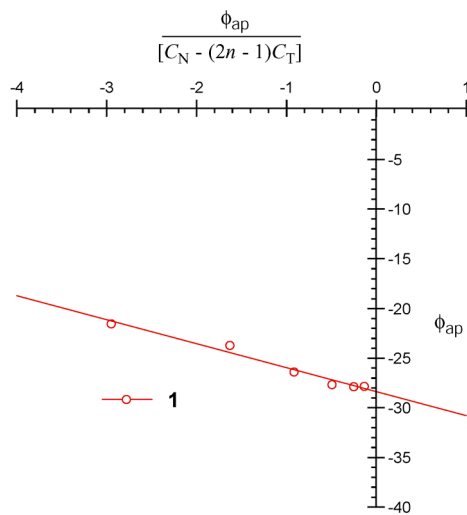


Figure 4.9 Unwinding plots for $\text{ImImPy-(R)}^{\text{H2N}}\gamma\text{-ImPyPy-}\beta\text{-C2-Phen-C2-}\beta\text{-PyPyIm-(R)}^{\text{H2N}}\gamma\text{-PyImIm}$ (**1**) on pUC19. Each data point was calculated from one set of topoisomer distributions from reactions containing polyamide compared to a control distribution lacking polyamide. Interception of the ordinate yields the unwinding angle (ϕ) per polyamide-TO conjugate.

Discussion

Here we show that bis-polyamide-phenoazone conjugates are capable of selectively binding to both 12 bp and 14 bp target sites on DNA. Of the series, the compound containing the shortest linker **1** binds with the highest affinity to the designed 12 bp match site, while compound **2** binds with the highest affinity to the designed 14 bp match site. Figure 4.10 shows a model of **2** bound to a 14 bp sequence of DNA. The model was derived from the NMR structure of actinomycin D³² and polyamide crystal structure³³ where the backbone of each DNA helix was properly overlaid and the linker region between the two moieties was energy minimized. By inspection, the linker for the 14 bp binding site appears to fit within the minor groove without significant DNA distortion, which is in agreement with the binding data presented above. A similar model for compound **1** (data not shown) implies that the 12 bp match site would best accommodate the conjugate, also in agreement with the affinity data. The lack of binding specificity at site **I** in either fragment suggests that the conserved

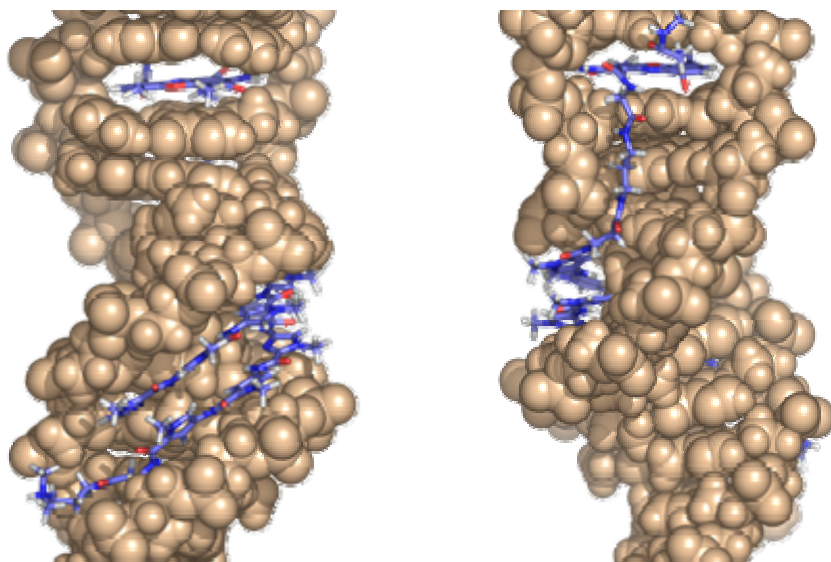


Figure 4.10 Composite modeling from both actinomycin D and polyamide homodimer DNA crystal structures, showing the C2 bis-polyamide-intercalator conjugate **1** bound to a 12 bp site.

region of the actinomycin D pentapeptide is bound in an unnatural orientation, which prevents formation of the essential hydrogen bond to guanine required for GC specificity. The manner in which the intercalator and polyamide are linked may also play a part in the lack of specificity at the intercalation site. Actinomycin D naturally links the phenoazone chromophore to the N-terminus of each peptide, but in our model the intercalator is initially linked to the N-terminus through the glycine tether then transferred to the C-terminus of the polyamide β -alanine residue through an aliphatic linker. The outcome of this arrangement is not fully understood, yet it is clear that the GC intercalation site is well tolerated. Finally, the unwinding data support the model of intercalation by showing an average unwinding angle within 1.5° of the natural product. The similar unwinding values suggest a comparable mode of binding for the phenoazone chromophore in both actinomycin and conjugate **1**.

To date, this new series of sequence-specific polyamide-intercalator conjugates favorably binds to the largest target sites of its class. It's not unreasonable to consider using larger hairpin polyamide motifs, such as eight-ring or $2\text{-}\beta\text{-}2$,³⁴ in a bis-polyamide-

phenoxazone context to further expand the binding site size and decrease the number of unwanted binding events. Such added specificity of this new bifunctional design may translate into less cytotoxicity when compared to the natural product.

Experimental

Materials

9-Chloroacridine was purchased from Pfaltz & Bauer, Inc. Restriction endonucleases were purchased from New England Biolabs and used as noted in the manufacturer's protocol. Sequenase (version 2.0) was obtained from Boeringher-Mannheim. [$\gamma^{32}\text{P}$]-Adenosine-5'-triphosphate (≥ 6000 Ci/mmol) was obtained from ICN. Purified pUC19 DNA for unwinding angle determination was isolated from transformed JM109 *Escherichia coli* using the Qiagen protocol. EDTA, dithiothreitol (DTT), ultrapure agarose, and calf thymus Topo I were purchased from GIBCO/BRL. Micron 50 microconcentrators were purchased from Amicon. ProbeQuant G-50. Micro Columns were purchased from Amersham Pharmacia Biotech, Inc. Water ($18\text{ M}\Omega$) was obtained from a Millipore MilliQ water purification system, and all buffers were $0.2\text{ }\mu\text{m}$ filtered. Reagent-grade chemicals were used as received unless otherwise stated.

UV spectra were measured on a Beckman-Coulter DU7400 diode array spectrophotometer. Matrix-assisted, laser desorption/ionization time-of-flight mass spectrometry (MALDI-TOF) was performed using an Applied Biosystems Voyager DE-Pro. HPLC analysis was performed on a Beckman Gold system using a RAININ C₁₈, Microsorb MV, $5\text{ }\mu\text{m}$, 300×4.6 mm reversed-phase column in 0.1% (v/v) TFA with acetonitrile as eluent and a flow rate of 1.0 mL/min. Preparatory reversed-phase HPLC was performed on a

Beckman HPLC using a Waters DeltaPak 25 × 100 mm, 100 μm C₁₈ column equipped with a guard, 0.1% (wt/v) TFA, 0.25% acetonitrile/min.

ImImPy-(R)^{H2N} γ -ImPyPy- β -C2-Phen-C2- β -PyPyIm-(R)^{H2N} γ -PyImIm (1)

Compound **8** (1 μmol aliquot) was dissolved in 500 μL of DMSO. To this solution was added diacid **7** (0.75 eq, 0.33 mg), PyBop (2 eq, 1.0 mg) and 5 μL of DIEA, and the reaction was allowed to proceed at room temperature for 1 h. The mixture was then treated with 1 mL of 80% TFA/DCM, 0.4 M PhSH. After 15 min the mixture was diluted with 0.1% (wt/v) TFA and the resulting solution purified by reversed-phase HPLC. Lyophilization provided ImImPy-(R)^{H2N} γ -ImPyPy- β -C2-Phen-C2- β -PyPyIm-(R)^{H2N} γ -PyImIm (**1**) as a yellow powder (100 nmol, 10% recovery). MALDI-TOF-MS (monoisotopic) calcd for C₁₀₄H₁₂₀N₄₂O₂₂ (M+H): 2311.3. Found: 2311.2.

ImImPy-(R)^{H2N} γ -ImPyPy- β -C3-Phen-C3- β -PyPyIm-(R)^{H2N} γ -PyImIm (2)

Synthesized as described for **1** starting from 1 μmol of **9** (150 nmol, 15% recovery). MALDI-TOF-MS (monoisotopic) calcd for C₁₀₆H₁₂₄N₄₂O₂₂ (M+H): 2339.4. Found: 2340.1.

ImImPy-(R)^{H2N} γ -ImPyPy- β -C4-Phen-C4- β -PyPyIm-(R)^{H2N} γ -PyImIm (3)

Synthesized as described for **1** starting from 1 μmol of **10** (110 nmol, 11% recovery). MALDI-TOF-MS (monoisotopic) calcd for C₁₀₈H₁₂₈N₄₂O₂₂ (M+H): 2367.4. Found: 2368.2.

ImImPy-(R)^{H2N} γ -ImPyPy- β -Me (4)

ImImPy-(R)^{NHFmoc} γ -ImPyPy- β -Pam-resin was generated from Boc- β -alanine Pam resin (1 g, 0.59 mmol/g) using previously described Boc-protected monomers and methods.²⁶ A sample of this resin (200 mg, 0.356 mmol/g) was suspended 0.1 M methyl amine in a

sealed container and heated (55°C) with periodic agitation for 16 h. The reaction mixture was filtered to remove resin, 0.1% (wt/v) TFA added (6 mL), and the resulting solution purified by reversed-phase HPLC. $\text{ImImPy-}(R)^{\text{NH2}}\gamma\text{-ImPyPy-}\beta\text{-Me}$ (**1**) was recovered upon lyophilization of the appropriate fractions as an off-white powder (18 mg, 16% recovery). MALDI-TOF-MS (monoisotopic) calcd for $\text{C}_{41}\text{H}_{50}\text{N}_{18}\text{O}_8$ ($\text{M}+\text{H}$): 923.9. Found: 923.8.

Glycine-2-nitro-3-benzyloxy-4-methylbenzamide (5)

Synthesized as previously described.²⁷

Glycine-2-amino-3-hydroxy-4-methylbenzamide (6)

Glycine-2-nitro-3-benzyloxy-4-methylbenzamide **5** (500mg, 1.5 mmol) was added to 250 mL methanol containing 70 mg 10% Pd/C, and the mixture was stirred under 1atm H_2 for 3 h. The solution was filtered through celite and the collected mixture carried on to **7** without further purification.

di-glycine-phenoxazone (7)

The solution of **6** above was added equal volume phosphate buffer (10 mM, pH 7.4). Upon addition of $\text{K}_3\text{Fe}(\text{CN})_6$ (1 g, 3 mmol) the solution instantly turned dark red. Stirring was continued for 1 hr and the methanol was removed *in vacuo*. The remaining solution was acidified to pH 3 with 1 M HCl, and the precipitate was filterd and dried to provide 210 mg (63% yield) of **7** as a fine red powder. Electrospray-MS calcd for $\text{C}_{20}\text{H}_{18}\text{N}_4\text{O}_8$ ($\text{M}+\text{H}$): 443.1. Found: 442.9.

$\text{ImImPy-}(R)^{\text{NHBOC}}\gamma\text{-ImPyPy-}\beta\text{-C2-NH}_2$ (8)

A sample of ImImPy-(*R*)^{NHFmoc}γ-ImPyPy-β-Pam-resin (150 mg, 0.356 mmol/g) was suspended in 4 mL of 4:1 piperidine-DMF and agitated (22°C, 30 min). The resultant ImImPy-(*R*)^{H2N}γ-ImPyPy-β-Pam-resin was washed sequentially with DCM and DMF. The resin was then suspended in 4 mL of NMP to which was added 500 mg of Boc₂O followed by 1 mL of DIEA, and the mixture was agitated (55°C, 30 min). The resultant ImImPy-(*R*)^{NHBoc}γ-ImPyPy-β-Pam-resin was washed sequentially with DMF, DCM, MeOH, and ethyl ether, and the amine-resin was dried in vacuo. A sample of resin was then treated with neat ethylenediamine (2 mL) and heated (55°C) with periodic agitation for 16 h. The reaction mixture was filtered to remove resin, 0.1% (wt/v) TFA added (6 mL), and the resulting solution purified by reversed-phase HPLC. ImImPy-(*R*)^{NHBoc}γ-ImPyPy-β-C2-NH₂ (**8**) was recovered upon lyophilization of the appropriate fractions as an off-white powder (8 mg, 17% recovery). MALDI-TOF-MS (monoisotopic) calcd for C₄₇H₆₂N₁₉O₁₀ (M+H): 1053.1. Found: 1053.8.

ImImPy-(*R*)^{NHBoc}γ-ImPyPy-β-C3-NH₂ (**9**)

Synthesized as described for **8** using neat 1,3-diaminopropane (2 mL) for polyamide cleavage from resin (9 mg, 16% recovery). MALDI-TOF-MS (monoisotopic) calcd for C₄₈H₆₃N₁₉O₁₀ (M+H): 1067.1. Found: 1067.4.

ImImPy-(*R*)^{NHBoc}γ-ImPyPy-β-C4-NH₂ (**10**)

Synthesized as described for **8** using neat 1,3-diaminobutane (2 mL) for polyamide cleavage from resin (11 mg, 17% recovery). MALDI-TOF-MS (monoisotopic) calcd for C₄₉H₆₅N₁₉O₁₀ (M+H): 1081.2. Found: 1081.6.

Construction of Plasmid DNA

The plasmid pEF18 and pEF19 was constructed by insertion of the following hybridized inserts into the *Bam*HI/*Hin*DIII polycloning sites in pUC19: 5'- GATCG TATGC CAGCT GGCAT ACGCA GCTAT CCCAG CTGGG ATACG CAGCT ATGCC ATATG GCATA GC -3' and 5'- AGCTG CTATG CCATA TGGCA TAGCT GCGTA TCCCA GCTGG GATAG CTGCG TATGC CAGCT GGCAT AC -3' for pEF18 and 5'- GATCG TATGC CATGC ATGGC ATACG CAGCT ATCCC ATGCA TGGGA TACGC AGCTA TGCCA TATAT GGCAT AGC -3' and 5'- AGCTG CTATG CCATA TATGG CATAG CTGCG TATCC CATGC ATGGG ATAGC TGCCT ATGCC ATGCA TGGCA TAC -3' for pEF19. The insert was obtained by annealing complementary *Hin*DIII restriction fragments of pUC19 using T4 DNA ligase. The ligated plasmid was then used to transform JM109 subcompetent cells (Promega). Colonies were selected for α -complementation on 25 mL Luria-Bertani agar plates containing 50 mg/mL ampicillin. Cells were harvested after overnight growth at 37°C. Large-scale plasmid purification was performed using WizardPlus Midi Preps from Promega. The presence of the desired insert was determined by dideoxy sequencing.

Preparation of 5'-End-Labeled Fragments

Two 21 base-pair primer oligonucleotides, 5'-GAATT CGAGC TCGGT ACCCG G-3' (forward) and 5'-TGGCA CGACA GGTTC CCCGA C-3' (reverse) were constructed for PCR amplification. The forward primer was radiolabeled using $[\gamma^{32}\text{P}]$ -dATP and polynucleotide kinase followed by purification using MicroSpin G-50 columns. The desired DNA segment was amplified as previously described.²³ The labeled fragment was loaded onto a 7% nondenaturing preparatory polyacrylamide gel (5% cross-link), and the desired

276 base-pair band was visualized by autoradiography and isolated. Chemical sequencing reactions were performed according to published protocols.^{35,36}

Quantitative DNase I Footprint Titrations

All reactions were carried out in a volume of 400 μL according to published protocols.²³ Quantitation by storage phosphor autoradiography and determination of equilibrium association constants were as previously described.³⁷

Unwinding Angle and Intrinsic Association Constant Determination

Relaxation reactions and numeric analyses were all carried out as described.^{24,25} Minor variations to published protocols include two-dimensional gel electrophoresis carried out in 18 \times 20 cm 1% agarose casting units and imaged after ethidium bromide staining with a Typhoon 8600 variable mode imager and 610-nm band-pass filter. The Boltzman distribution of adopted integer Lk values were plotted using the equation (1),

$$I = I_M e^{[-w(\Delta Lk - \Delta Lk_c)^2]} \quad (1)$$

where ΔLk and ΔLk_c are the measured linking difference and most abundant linking difference, respectively, I and I_M are integrated and maximum band intensity, respectively, and w is the distribution width. The apparent unwinding angle was calculated using equation (2),

$$\phi_{ap} = \frac{360N_D(\Delta Lk_c - \Delta Lk^o_c)}{N_L} \quad (2)$$

where ΔLk^0_c is the most abundant linking difference for the control reactions containing no polyamide, and N_D and N_L are the number of pUC19 and polyamide conjugate molecules, respectively. The actual unwinding angle was calculated using equation (3),

$$\phi_{ap} = \phi - \frac{\phi_{ap}}{K_a[C_N - (2n - 1)C_T]} \quad , \quad (3)$$

where n represents the number of binding sites covered by one conjugate (set to unity), and C_N and C_T represent the concentration of conjugate binding sites and the concentration of polyamide conjugate, respectively. The value of C_N affects the slope in Figure 4.8 but does not influence the value of ϕ (ϕ is the ordinate intercept).

Acknowledgment

We are grateful to the National Institutes of Health (Grant 27681) for research support and a Research Service Award to E.J.F. We also thank the Ralph M. Parsons Foundation for a predoctoral fellowship to E.J.F.

References

1. Brockman, H. and J. Lackner, *J. Chem. Ber.* **1968**, 101, 1312.
2. Meienhofer, J., *J. Am. Chem. Soc.* **1970**, 92, 3771-3777.
3. Krugh, T. R. and M. A. Young, *Nature*, **1977**, 269, 627-628.
4. Takusagawa, F., M. Dabrow, S. Neidle, and H. M. Berman, *Nature*, **1982**, 296, 466-469.
5. Sobell, H. M. and S. C. Jain, *J. Mol. Biol.*, **1970**, 68, 21-34.
6. Patel, D. J., A. Pardi, and K. Itakura, *Science*, **1982**, 216, 581-590.
7. Krey, A. *FEBS Lett.*, **1973**, 26, 58.
8. Meienhofer, J. and E. Atherton, *Structure-Activity Relationship among the Semisynthetic Antibiotics*; Perlman, D., Ed.; Academic Press, Inc.: New York, 1977; pp 427-529.
9. Sobell, H. M., S. C. Jain, T. D. Sakore, and C. E. Nordman, *Nature, New Biol.* **1971**, 231, 200-205.
10. Sobell, H. M. and S. C. Jain, *J. Mol. Biol.* **1972**, 68, 21-34.
11. Fox, K. R. and M. J. Waring, *Nucl. Acids Res.*, **1984**, 9271-9284.
12. Van Dyke, M. W., R. P. Hertzberg, and P. B. Dervan, *Proc. Natl. Acad. Sci. USA* **1982**, 79, 5470-5474.
13. Van Dyke, M. M. and P. B. Dervan, *Nucl. Acids Res.*, **1983**, 11, 5555-5567.
14. Muller, W. and D. Crothers, *J. Mol. Biol.*, **1968**, 35, 251.
15. Devoe, H. and I. Tinoco, *J. Mol. Biol.*, **1962**, 4, 518.
16. Goldberg, J. H. and P. A. Friedman, *Annu. Rev. Biochem.* **1971**, 40, 775-810.
17. Kersten, H. and W. Kersten, *Inhibitors of Nucleic Acid Synthesis*; Springer Verlag: Berlin, 1974, pp 40-66.

18. Hurwitz, J., J. J. Furth, M. Malamy, and M. Alexander, *Proc. Natl. Acad. Sci. USA* **1962**, 48, 1222-1223.
19. Goldberg, I., M. Hobinowitz, and E. Reich, *Proc. Natl. Acad. Sci. USA* **1962**, 48, 2094.
20. Fechter, E. J. and P. B. Dervan, *J. Am. Chem. Soc.* **2003**, 125, 8476-8485.
21. Fechter, E. J., B. Olenyuk, and P. B. Dervan, *Angew. Chem. Int. Ed.* **2004**, 43, 3591-3594.
22. White, S., J. W. Szewczyk, J. M. Turner, E. E. Baird, and P. B. Dervan, *Nature* **1998**, 391, 468-471.
23. Trauger, J. W. and P. B. Dervan, *Methods Enzymol.* **2001**, 340, 450-466.
24. Zeman, S. M., K. M. Depew, S. J. Danishefsky, and D. M. Crothers, *Proc. Natl. Acad. Sci. USA* **1998**, 95, 4327-4332.
25. Zeman, S. M. and D. M. Crothers, *Methods Enzymol.* **2001**, 340, 51-68.
26. Baird, E. E. and P. B. Dervan, *J. Am. Chem. Soc.* **1996**, 118, 6141-6146.
27. Sluka, J. Doctoral Thesis **1988**, 125-176.
28. All relaxation reactions were run at a sufficiently high (and constant) binding site-to-polyamide ratio to ensure that unwinding effects were only caused by sequence-specific interactions.
29. Kielkopf, C. L., S. White, J. W. Szewczyk, J. M. Turner, E. E. Baird, P. B. Dervan, and D. C. Rees, *Science* **1998**, 282, 111-115.
30. Suto, R. K., R. S. Edayathumangalam, C. L. White, C. Melander, J. M. Gottesfeld, P. B. Dervan, and K. Lugar, *J. Mol. Biol.* **2003**, 326, 371-380.
31. Waring, M. *J. Mol. Biol.* **1970**, 54, 247-279.
32. Lian, C. H. Robinson, and A. H. J. Wang, *J. Am. Chem. Soc.* **1996**, 118, 8791-8801.

33. Kielkopf, C. L., S. White, J. W. Szewczyk, J. M. Turner, E. E. Baird, P. B. Dervan, and D. C. Rees, *J. Mol. Biol.* **2000**, 295, 557-567.
34. Wang, C. C. C., U. Ellervik, and P. B. Dervan *Bioorg. Med. Chem.* **2001**, 9, 653.
35. Maxam, A. M. and W. S. Gilbert, *Methods Enzymol.* **1980**, 65, 499-560.
36. Iverson, B. L. and P. B. Dervan, *Methods Enzymol.* **1996**, 15, 7823-7830.
37. Johnston, R. F., S. C. Pickett, and D. L. Barker, *Electrophoresis* **1990**, 11, 355-360.